

JPL Document D-1549543

TECHNOLOGY DEVELOPMENT FOR EXOPLANET MISSIONS

Technology Milestone #3 Whitepaper: Nulling of an Actively-Controlled Segmented Aperture Telescope

Brian Hicks (PI), Matthew Bolcar, Peter Petrone III, Michael Helmbrecht

August 17, 2016

National Aeronautics and Space Administration

Jet Propulsion Laboratory
California Institute of Technology
Pasadena, California

Approvals

Released by

Brian Hicks
Principal Investigator

Matthew Bolcar
Co-Investigator

Approved by

Nick Siegler
Exoplanet Exploration Program Chief Technologist, JPL

Douglas Hudgins
Exoplanet Exploration Program Scientist, NASA HQ

Contents

1	Objective	4
2	Introduction/Background	4
3	Milestone Definition	5
4	Experiment Description	6
4.1	Segmented Aperture Telescope	7
4.2	Visible Nulling Coronagraph	8
4.3	Additional Technologies	10
5	Data Measurement and Analysis	10
6	Success Criteria	11
6.1	Bandpass	12
6.2	Contrast	12
6.3	Confidence	12
6.4	Repeatability	12
7	System Architecture Needs	12
7.1	Mount ruggedization	12
7.2	Vacuum-compatible dark channel optics	14
7.3	A fully-functional segmented DM	14
7.4	Delay stage stabilization	15
7.5	Vacuum chamber modifications	16
7.6	Enhanced Fresnel rhomb achromatic phase shifters	16
7.7	Realtime operating system (RTOS) upgrade	16
7.8	Single mode fiber array (SFA) characterization	17
8	Schedule	17

Acronyms

APS Achromatic Phase Shifter
DCE - Data Collection Event
DM Deformable Mirror
GSFC Goddard Space Flight Center
HabEx - The Habitable Exoplanet Imager
HZ - Habitable Zone
IRAD Internal Research and Development
IWA Inner Working Angle
LUVOIR - Large UV/Optical/InfraRed
MEMS - Microelectromechanical Systems
MMA Multiple Mirror Array, a.k.a. (hex-packed) segmented MEMS DM
MPI - Message Passing Interface
PSF - Point Spread Function
PTT - Piston–Tip–Tilt (or piston, tip, and tilt)
PZT - Piezoelectric Transducer (or “piezo”)
RMS - Root Mean Square
RTOS Real Time Operating System
SAT Strategic Astrophysics Technology
SBIR Small Business Innovation Research
SAINT - Segmented Interferometric Interferometric Nulling Testbed
SFA Spatial Filter Array, or Single mode Fiber Array
TIR - Total Internal Reflection
TDEM Technology Development for Exoplanet Missions
TRL Technology Readiness Level
VNC Visible Nulling Coronagraph
WFC Wavefront Control
WFE - Wavefront Error
WFS Wavefront Sensing

1 Objective

In support of NASA’s Exoplanet Exploration Program and the Technology Demonstration for Exoplanet Missions (TDEM) component of NASA’s Strategic Astrophysics Technology (SAT) solicitation, we will demonstrate high-contrast imaging with the Visible Nulling Coronagraph (VNC) using a segmented aperture telescope. This is accomplished by combining the existing VNC testbed with a segmented primary mirror telescope to form the Segmented Aperture Interferometric Nulling Testbed (SAINT).

2 Introduction/Background

The direct detection and characterization of exo-Earths is predicated on having the light gathering power and angular resolution available with large telescopes. It additionally requires the ability to suppress starlight relative to the planet at small angular separations. The planet-to-star luminosity ratio in visible light versus angular separation is shown in Fig. 1 for candidate target stars out to 30 parsecs. In addition to highlighting the contrast challenge, Fig. 1 shows that, due to limited resolution, 1-2 meter apertures are incapable of detecting planets observed at quadrature in mean habitable zone (HZ) orbits around their parent stars, even when assuming an ambitious inner working angle (IWA) of $2\lambda/D$. Recent yield studies indicate that an aperture of 8 meters or greater is necessary to discover tens of HZ exo-Earths, thus allowing for a statistical analysis of the likelihood of habitability.[1] In 2018, the James Webb Space Telescope (JWST) will have the largest space telescope aperture at 6.5 meters. JWST is a deployable segmented aperture telescope designed to image first light targets. NASA’s investment in JWST will have an impact on future flight mission telescope architectures constrained by launch fairing size - large space telescopes will either need to be deployed or assembled. Thus, coronagraphy should be adept at operating on segmented apertures.

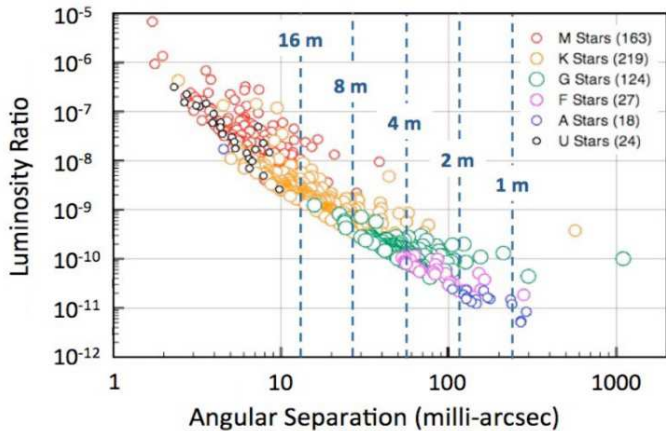


Figure 1: Candidate terrestrial exoplanet luminosity ratio vs. angular separation. Apertures from 1-16 meters are shown as blue dashed lines. Planets to the right of each dashed line are observable by that aperture, assuming a coronagraph inner working angle of $2\lambda/D$ and a V-band filter. The plot includes all stars out to a distance of 30 parsecs and assumes an Earth-sized terrestrial planet in the luminosity-corrected mean habitable zone. The number of candidates per spectral class is provided in the legend.

Due to their diffractive nature, most coronagraphic designs and demonstrations to date have used unobscured circular apertures, and nominally would operate with a large, off-axis telescope. Aperture masking approaches must trade throughput and IWA. Alternatively, a segmented aperture can achieve the same contrast as a filled-aperture but at greater angular separations, or specific focal plane locations; either of which lowers the potential number of targets. The diverse space of possible future flight apertures (Fig. 2) is not well-matched to the suite of focal plane mask coronagraphs undergoing significant technology development. While segmented apertures are not ideal for exoplanet coronagraphy, it is a path that needs further exploration to be better understood, as this effort proposes to do.

A key benefit of the VNC is that it is one approach that has been shown to be adaptable to a variety of apertures addressed during the Astrophysics Strategic Mission Concept (ASMC) studies. Three of the ASMC studies included a VNC (Fig. 2): the Extrasolar Planetary Imaging Coronagraph (EPIC) with a filled aperture[2], the Advanced Technology Large Aperture Space Telescope (ATLAST) with a segmented aperture[3], and the Dilute Aperture Visible Nulling Coronagraphic Imager (DAViNCI) with a sparse aperture[4].

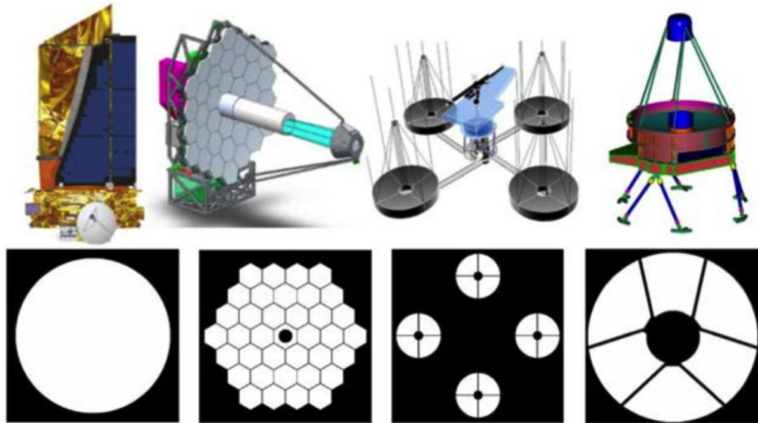


Figure 2: The VNC has been studied for several exoplanet missions that span the range of apertures. EPIC (left) is a 1.65-m probe-class mission concept to image and characterize exoplanet environments. ATLAST (left-center) and DAVINCI (right-center) are flagship-class mission concepts designed to image and characterize terrestrial exoplanets. WFIRST (right) is the next flagship mission to follow JWST and will include a coronagraph instrument capable of directly imaging gas giant planets. The bottom row shows the aperture shape for each mission.

Evaluations of segmented apertures, sensing/control, and telescope stability show that the VNC leads to a viable and manageable approach for a flight mission[5, 6]. This led to the Discovery mission proposal for EPIC[2]. To further evaluate the approach and sub-system-level technologies, a VNC laboratory testbed was developed at GSFC that has achieved a milestone in nulling coronagraphy (Fig. 3). This narrow band laboratory work with the VNC achieved repeatable contrasts of 5.5×10^{-9} at an IWA of $2\lambda/D$ while operating under closed-loop control with a segmented deformable mirror.[7] Unlike other traditional coronagraphs, this contrast result is the first high contrast demonstration with a segmented deformable mirror (DM), and the deepest known nulling of any interferometer to date. The VNC testbed, as it stands now, has not been coupled to a telescope, but exists as a stand-alone laboratory testbed for evaluating nulling coronagraphy, sensing and control, and critical technologies including the deformable mirror (DM) and achromatic phase shifter (APS).

We will advance the VNC for a segmented aperture telescope by integrating the existing laboratory VNC with another existing, but modified, testbed known as the Fizeau Interferometry Testbed (FIT).[8] FIT was initially constructed to evaluate wavefront control for the Stellar Imager (SI) mission[9], and has been modified to include a seven-segment actuated primary mirror (see Sec. 4.1). An existing fast-steering mirror (FSM) will also be incorporated to allow for demonstrations of pointing-error control. The combination of the VNC, the modified FIT, and the FSM comprise the Segmented Aperture Interferometric Nulling Testbed (SAINT). The effort will culminate in a demonstration of an end-to-end segmented aperture system with high-contrast imaging. We will work to achieve a contrast of 10^{-8} at an IWA of $4\lambda/D$ and spectral bandpass of 20 nm centered on 633 nm. It is likely that SAINT can reasonably achieve 10^{-9} contrast at a smaller IWA, possibly $\sim 3\lambda/D$, however we adopt the conservative approach since this is the first time the VNC will have been connected to a segmented aperture; we carry the deeper contrast at smaller IWA as a stretch goal.

This effort completes a key milestone that further advances coronagraphy towards being adaptable to arbitrary apertures, thereby freeing up the necessity of requiring unobscured off-axis telescopes, and takes a significant step towards coronagraphy becoming viable for any telescope. This may result in overall mission cost savings in that either existing telescopes, or telescopes designed and optimized for other science projects could be made available for exoplanet science missions.

3 Milestone Definition

Baseline demonstrations of narrowband and broadband performance will be performed according to the Milestone Definitions and Success Criteria established in the associated VNC TDEM Milestone #1 and Milestone #2 reports.[7, 10]. Results from these demonstrations will be reported to the TAC for review as intermediate Milestones #1.5 and #2.5, respectively, before proceeding to the Milestone #3 SAINT

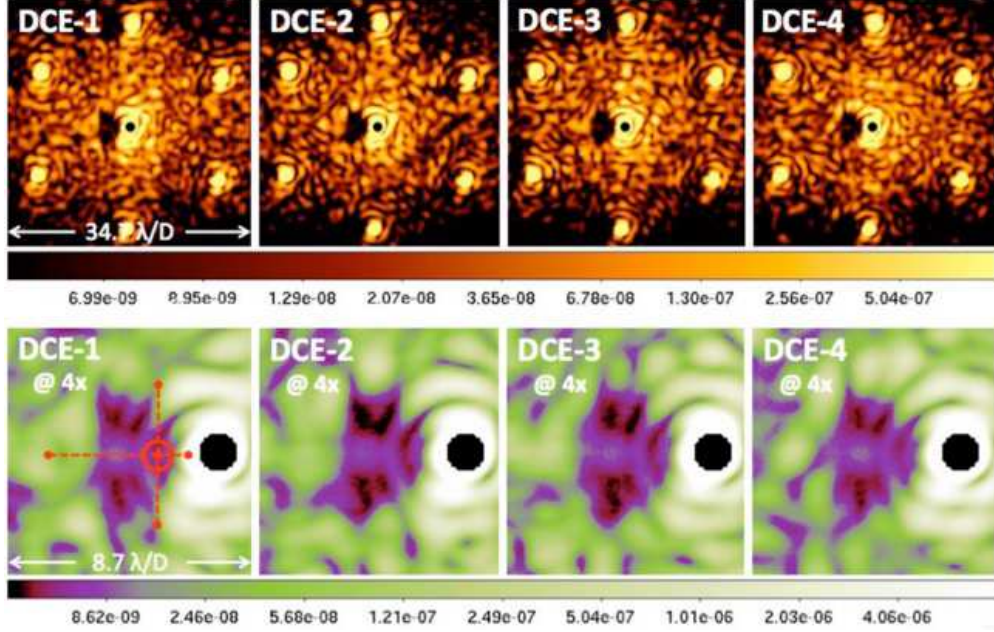


Figure 3: Contrast maps from the VNC TDEM (narrowband) Milestone #1. The top row shows the resulting average contrast maps from four different data collection events (DCE) on a log and color stretched scale to show residual structure. The bottom row shows the same images as the top, but zoomed by a factor of 4 and with a different color map to accent the dark-hole region. The central core (dark circle) is numerically masked to compress the image dynamic range for display purposes. The open red circle on the lower left panel shows a $1\lambda/D$ diameter region centered on $2\lambda/D$ this is the region over which contrast was calculated for this milestone.

demonstration.

Milestone #3 is succinctly stated as achieve and hold a contrast of 10^{-8} at an IWA of $4\lambda/D$ within a bandpass of $\Delta\lambda = 20$ nm centered at 633 nm for 1,000 seconds on three separate occasions, with a goal of 10^{-9} at an IWA of $3\lambda/D$ in a bandpass of $\Delta\lambda = 40$ nm. *Achieve and hold* means that multiple 10^{-8} or better contrast measurements will be measured during each 1,000 second period. The milestone addresses broadband contrast measurement and broadband wavefront control for a segmented aperture. Our proposed effort leverages the lessons learned from completing the first TDEM milestone of 10^{-8} contrast at an IWA of $2\lambda/D$ on three separate occasions.[7]

4 Experiment Description

The milestone is accomplished by first modifying the existing FIT sparse aperture testbed to convert it to a segmented telescope with reconfigurable aperture patterns. The actuated FIT sparse aperture array has been replaced with seven hexagonal primary mirror segments (a ring of six segments with a removable or maskable central, seventh segment). Each segment is separately bonded to flexure-mounted piezo actuators that attach to the back-plane structure. Construction of the segmented primary mirror has been completed, and was funded under GSFC Internal Research and Development (IRAD). SAINT represents an effective leveraging strategy since primary costs for this effort are to integrate the SAINT components (VNC, segmented telescope, FSM) and perform the contrast measurements.

The Lyot mask for the SAINT end-to-end system is shown in the left panel of Fig. 4, formed by the union of an Iris AO, Inc. PTT489 MMA (a device with 163 segments corresponding to seven hexagonal array rings less vertices) with the SAINT seven segment hexagonal primary mirror. A cross-section of the corresponding PSF (the right panel of Fig. 4 with intensity stretched as $I^{1/4}$) is shown in the central panel of the same

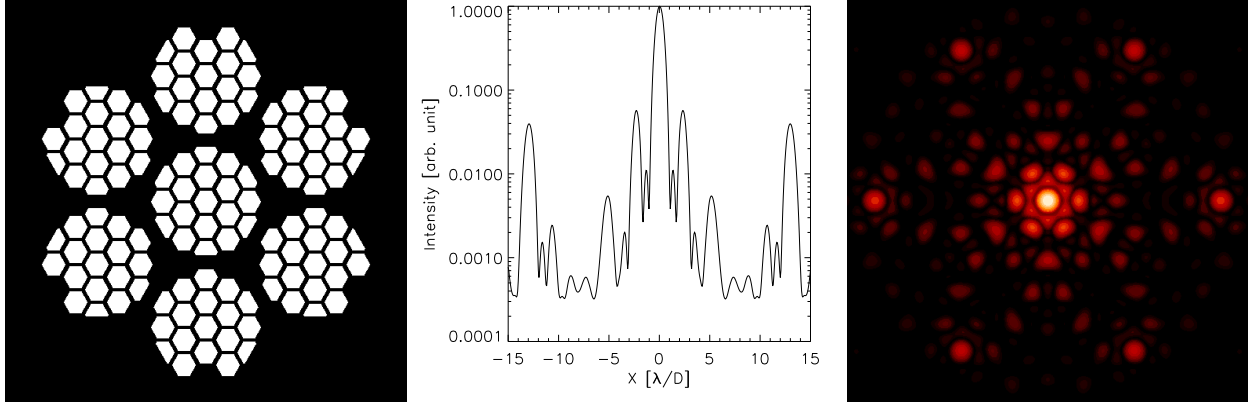


Figure 4: The SAINT Lyot mask (left) and corresponding cross-section (center) and $I^{1/4}$ stretch (right) of the PSF showing inner and outer sidelobes attributed to the SAINT primary and the seven-ringed MMA hexagonal array.

figure. Inner sidelobes at $3\lambda/D$ are attributed to the SAINT primary. The outer sidelobes are attributed to the seven-ringed MMA hexagonal array. Segments that span primary mirror gaps will be masked out and not controlled, leaving a total of 127 controllable segments. An e-beam deposition or photolithographic Lyot mask fabrication process will increase segment subaperture throughput by as much as 80% of the current throughput (i.e., $1.8\times$ increase in area).

The milestone represents a feasible objective, and is based on current VNC Technology Readiness Levels (TRLs), and the TRL of component technologies, including: wavefront control for segmented apertures (per JWST), DMs, and APS. This effort is an important step towards enabling exoplanet coronagraphy for segmented apertures and ultimately for future missions such as a Large UV/Optical/Infrared (LUVOIR) Surveyor or the Habitable Exoplanet Imager (HabEx). Upon completion of this two-year effort, sub-system technology will be properly positioned to address the additional steps required to mature this high-contrast imaging approach to TRL 6.

Our team has the facilities and software tools required to successfully complete this effort. The VNC testbed has demonstrated active nulling under closed-loop control within the tank. Additionally, a 100% yield DM has been procured via NASA Small Business Innovative Research (SBIR) awards and is ready to replace the current DM which, despite having several failed actuators, was used during the first VNC demonstrations.

Fig. 5 shows a layout of the SAINT optical system. A 16×4 stabilized air table supports the system, which consists of a source module and the segmented aperture telescope (see Fig. 6) in an enclosure, and a vacuum chamber containing the VNC. Fig. 7 shows the VNC outside of the chamber on an adjacent table used for integration and alignment. A control system consisting of a control computer, electronics, device drivers are being upgraded to run in a real time operating system (RTOS) version of Linux running C with message passing interface (MPI) for threading across multiple processors. The control electronics are isolated from the floating air table, although some additional isolation and modifications to the vacuum tank are necessary to mitigate existing mechanical shorts (Sec. 7). Underneath the feet of the vacuum tank are passive isolators, and within the tank, the VNC itself rests on a shelf on a 3-point passively-isolated mount. In the following sections we describe the components of SAINT and the proposed laboratory work.

4.1 Segmented Aperture Telescope

An actuated, hexagonally-segmented, spherical primary mirror (PM) is used as input to the VNC. Each segment is mounted onto piezo-actuated flexures, allowing control of each segment in three degrees of freedom (piston, tip, and tilt). The PM is the aperture stop and entrance pupil of SAINT. Two conic secondary mirrors are included in the optical train, and are designed to correct the spherical aberration and astigmatism

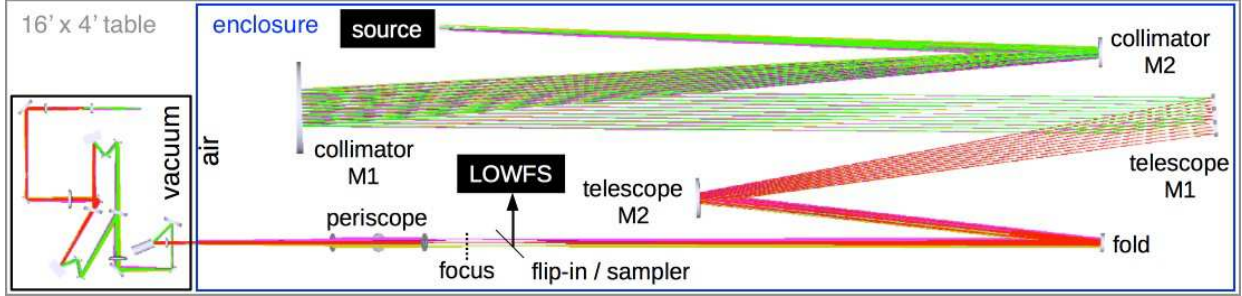


Figure 5: An end-to-end raytrace of the Segmented Aperture Interferometric Nulling Testbed (SAINT) consisting of 4 primary subsystems: (i) Source Module, (ii) Segmented Aperture Telescope, (iii) Visible Nulling Coronagraph, and (iv) Control System (not shown). SAINT will demonstrate high-contrast imaging with a segmented telescope, develop coupled sensing and control, and assess closed-loop contrast and inner working angle over a finite spectral bandpass of $\Delta\lambda = 20$ nm centered on 633 nm. The optics are shown to scale, and the table, vacuum chamber, and enclosure are shown approximately to scale. A pupil is traversed each time the ray bundle changes color from predominantly red to green and vice versa.

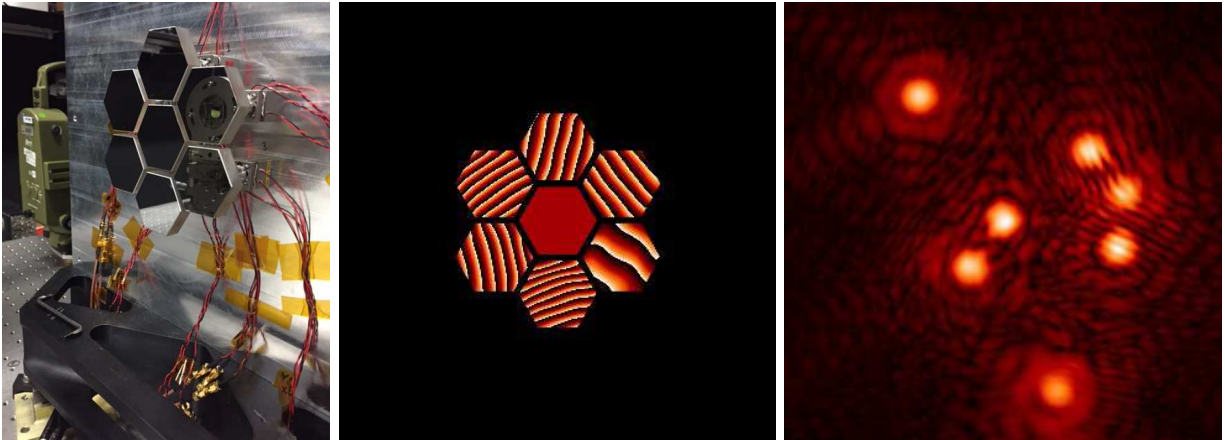


Figure 6: The SAINT M1 mounted and coarse-aligned on its backplane (left), a simulation of surface errors and residual tilt fringes observed in the pupil plane to be removed through piezo actuation (center), and the corresponding PSFs associated with each segment prior to coherent phasing (right).

of the spherical segments, and coma from the parabolic collimator. Bypass optics are also included to allow source module light to directly enter the VNC without passing through the telescope allowing each to be independently aligned and operated for debugging purposes, prior to operating the end-to-end system. All of the optics and mounts and segment actuators for the segmented aperture telescope have been procured and are assembled and are already available to this effort.

A relay images the entrance pupil to a pupil on the FSM (see Fig. 7) to mitigate pointing drift and jitter between the telescope and VNC. An intern, funded through the GSFC Education Office, has begun work on the fine pointing system, and will continue developing it during the summer of 2016 at no cost to this effort.

4.2 Visible Nulling Coronagraph

The VNC uses a combination of active and passive components to achieve the desired contrast at small IWA over a finite spectral bandpass. In its most simplistic form it works by destructive and constructive interference: placing a star on the destructive interference central minimum (null) moves the stars light from the science channel to the bright pupil camera for wavefront and fine pointing control. Conversely,

placing the planet on a constructive interference maximum allows transmission of the planet light to the dark science camera. The left panel of Fig. 7 shows a photo of the existing VNC, and the right panel shows a raytrace and schematic of modifications being made to imaging and relay optics, including the fine pointing system. Fore-optics re-image the pupil at the FSM to the coronagraph. The beamsplitter/combiner (BS/C) separates the two arms of the interferometer. A segmented deformable mirror (labeled PTT489 in Fig. 7) corrects non-common path errors between the arms. The reference arm contains a delay mechanism which equalizes the path length between the two arms. Shutters and linear polarizers in each arm (not shown in the raytrace) are used to measure and balance amplitude, respectively.[11, 7] Aft-optics relay the bright and dark output beams to wavefront sensing and science cameras, respectively. The Fresnel rhomb APS optics are shown in Fig. 9.

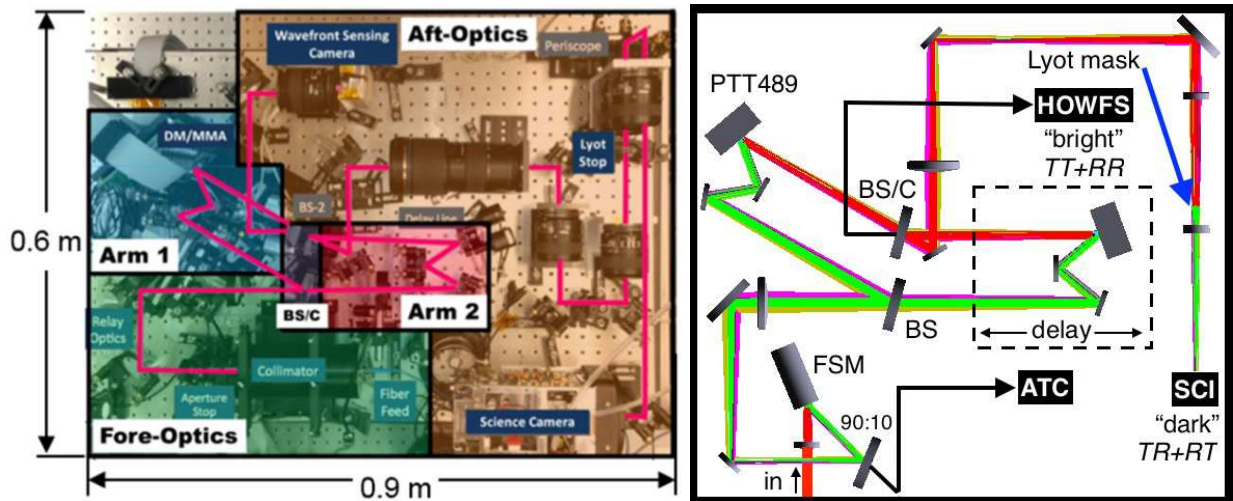


Figure 7: The VNC fits compactly on a single breadboard. Fore-optics used to collimate and relay a fiber-fed point source for injection into the nuller will be replaced by optics that accommodate a beam fed to the system through a vacuum window. A pick-off sends light to an angle tracker camera (ATC) to provide feedback for a fast steering mirror (FSM) for pointing stabilization between the VNC and the external source feed. The simplified aft-optics shown in the raytrace relay the nuller outputs to the bright and dark channel cameras. As in Fig. 5, a pupil is traversed each time the ray bundle changes color from predominantly red to green and vice versa. Shutters, polarizers, and the Fresnel rhomb APS present in each arm of the nuller are not shown.

Both the fore-optics and aft-optics will be reworked as part of the SAINT development. The fore-optics will be modified to include the fine-steering mirror and tracking camera for pointing control. The aft-optics will be simplified to remove the existing zoom lenses, folds, and periscopes to a straightforward relay from the dark channel output to the Lyot stop and then to the dark channel science camera. This will not only improve robustness and stability of the instrument, but remove significant chromatic aberration that is present in the existing aft-optics.

Vacuum feed-throughs consisting of electrical cables and water-chiller lines pass through a tank bulkhead. An optical port, consisting of a vacuum window, on a second tank bulkhead allows for the light from the external segmented aperture telescope to be coupled to the VNC inside the vacuum tank.

The VNC provides, via its interferometer signal, all of the outputs required to track pointing jitter, to move and control the FSM, and to sense and control the segment level wavefront error, and the residual non-common path error (via the DM). Perhaps the most important advantage of the VNC is that it can null to high contrast using the starlight from the centrally nulled star and the residual speckle in the science image.

4.3 Additional Technologies

Multiple Mirror Array (MMA)

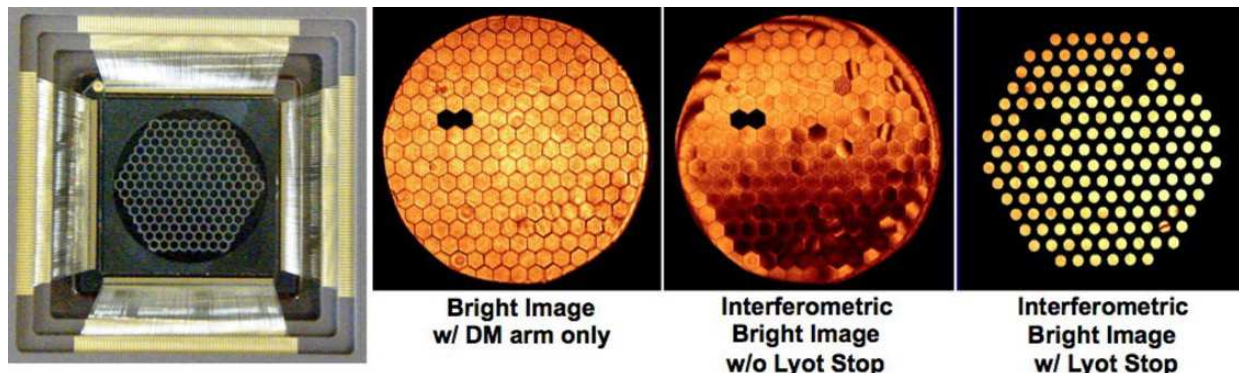


Figure 8: (Left) Photo of the MMA used in VNC Milestones #1 and #2 and images of the device observed using the bright output pupil camera with one arm of the VNC blocked (Left-Center), with both arms open showing interference fringes (Right-Center) and imaged through the Lyot stop (Right). Five inactive segments are masked out. This MMA will be replaced with a fully-functional MMA having all active segments. A new SAINT Lyot mask resembling what is shown in the left panel of Fig. 4 will be fabricated in this effort.

The MMA is a hexagonally-packed segmented MEMS deformable mirror developed under a phase-II SBIR with Iris AO, Inc., and consists of 163 segments (Fig. 8), of which 5 are inoperable and masked out with the Lyot stop. Each segment is actuated in the three degrees-of-freedom of piston, tip, and tilt, and can move over the range of 0 to 1 μm in piston, and ~ 200 arcseconds in tip and tilt. The MMA was delivered to GSFC in May of 2010 and integrated into the VNC and has been operational on a daily basis. Each of the MMA segments is 606.22 μm flat-to-flat with gaps of 45 μm . This MMA consists of single crystal silicon, coated with protected aluminum and have $\sim 2 - 4$ nm RMS surface error. The full width (from left to right) of the longest row of segments is 9.2 mm. This MMA that has been employed in recent milestone efforts will be replaced with a fully-functional DM that has been kept in reserve for this Milestone #3 effort.

Achromatic Phase Shifter

The APS is detailed in [12] and works by using two pairs of Fresnel rhomb prisms, with one prism pair per arm and clocked 90° in one arm relative to the other (Fig. 9). The APS is an all-glass device that exploits the achromaticity of the phase difference between the s- and p-polarization states to perform achromatic nulling. The use of the APS allows both broadband and high throughput nulling due to anti-reflective coatings on the input/output facets and total internal reflection at the phase-shifting facets. It will be employed in SAINT to demonstrate broadband dark holes with a segmented aperture telescope.

5 Data Measurement and Analysis

After the integration of SAINT, a series of calibration data sets will be collected. The first will use the SAINT bypass optics that relays source module light directly into the VNC, bypassing the segmented aperture telescope. A contrast measurement will be collected in this configuration to verify that modifications to the VNC itself (e.g. movement of the source module outside the tank, inclusion of the FSM and tracking camera, etc.) have not negatively impacted the fundamental performance of the instrument.

A second calibration measurement will be made using just the source module and segmented aperture telescope, relaying the telescope focal plane directly to a phase retrieval camera, excluding the VNC instrument. Image plane wavefront sensing techniques will be used to verify phasing of the segmented aperture telescope PM.

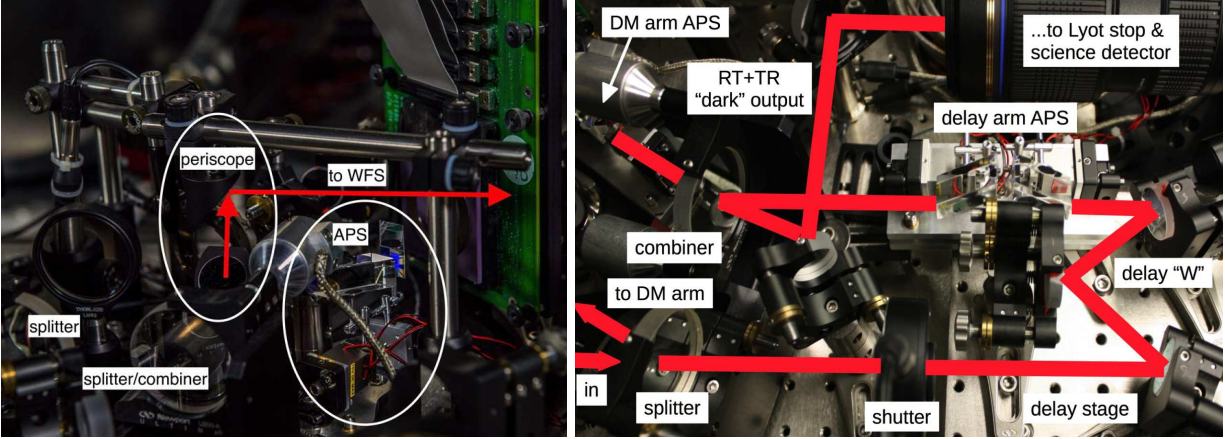


Figure 9: Fresnel rhomb prisms provide an achromatic π -phase shift to each polarization through total internal reflection, enabling broadband nulling of the starlight. The rhombs pairs are clocked 90° with respect to each other in the DM arm (Left) and the delay arm (Right)

Finally, the two systems will be coupled and experiments will begin to achieve the Milestone as defined in Sec. 3. This demonstration will incorporate all aspects of the SAINT testbed, and will rely on the wavefront control system to actively control all degrees of freedom, including: piston, tip, and tilt on each of the seven PM segments; tip and tilt of the FSM; piston of the VNC delay-arm mechanism; piston, tip, and tilt of each of the active DM segments; and available pitch, roll, and yaw degrees of freedom on each of the APS prisms.

Collection of all contrast data sets will be similar in practice to the demonstrations performed as part of the first VNC TDEM milestone.[7] The calculations of the contrast metric and confidence limits will be performed according to established Program guidelines. The following data or data images will be presented in the intermediate Milestones #1.5 and #2.5, as well as the Milestone #3 Final Report:

1. Model predictions of contrast performance including effects of bandpass, optical surfaces, static and dynamic misalignment, and a comparison of single mode fiber array (SFA) bundle versus Lyot mask filtering, followed by revised post-demonstration analysis
2. Calibrated images of the reference on-axis PSF (i.e. star)
3. The coronagraph focal plane scale and calibrated spectral filter function
4. A set of three independent Data Collection Events (DCEs); including all contrast realization images therein
5. A contrast metric value for the target area for each of the DCEs
6. A statistical analysis of contrast values, with 90% confidence contrast value for the total data set
7. A histogram and cumulative histogram of the brightness distribution of pixels in the dark field for each of the contrast realization images, for each of the DCEs

These source will be made available to the Exoplanet Exploration Program.

6 Success Criteria

Listed are the required elements of the milestone demonstration with its rationale.

6.1 Bandpass

A baseline filter of 20 nm FWHM centered on 633 nm will be used. This filter will be calibrated with a lab spectrophotometer to measure its transmittance at 1 nm resolution. The baseline filter shall serve as the reference filter for future measurements.

Rationale: This filter will restrict the bandpass of observation to the milestone objective. The filter serves the same role as one would on a space mission.

6.2 Contrast

A mean contrast metric of 1×10^{-8} or smaller shall be achieved in a region extending from $3.5 - 4.5\lambda/D$, centered on $4\lambda/D$ in the focal plane for using the 20 nm FWHM spectral filter.

Rationale: This provides evidence that the high-contrast field is sufficiently dark to be useful for searching for planets.

6.3 Confidence

Criterion 6.3, averaged over each of three DCEs shall be met with a confidence of 90% or better. Sufficient data will be taken to justify this statistical confidence.

Rationale: Assuming the contrast values have a Gaussian distribution about the mean contrast, this demonstrates a statistical confidence of 90% that the mean contrast goal has been reached.

6.4 Repeatability

Elements 6.1-6.3 must be satisfied on three separate occasions with a reset of the wavefront control system software (DM set to scratch) between each demonstration.

Rationale: This provides evidence of the repeatability of the contrast demonstration. The wavefront control system software reset between each data sets ensures that the three data sets can be considered as independent and do not represent an unusually good configuration that cannot be reproduced. For each demonstration the DM will begin from a scratch setting and the algorithm used to converge will have no memory of settings used for prior demonstrations. There is no time requirement for the demonstrations, other than the time required to meet the statistics stipulated in the success criteria. There is no required interval between demonstrations; subsequent demonstrations can begin as soon as prior demonstrations have ended. There is also no requirement to turn off power, open the vacuum tank, or delete data relevant for calibration of the DM influence functions.

7 System Architecture Needs

Known issues that have been identified as being hindrances to reaching the broadband Milestone in this effort are described below and summarized in Tab. 1. Addressing these issues will be carried out pending continued funding through, e.g., SAT/TDEM and/or GSFC IRAD awards.

7.1 Mount ruggedization

While it has been the claim that one of the major advantages of the VNC approach to WFC is observation through the control sequence, this relies on trades between control rates and the power spectrum of perturbances, which is a net sum of slow thermal and (induced) electrical drifts, as well as sustained and impulsive mechanical and acoustical disturbances.

Improving ruggedness minimizes time lost to realignment of optics, which can also necessitate that the digital

Table 1: Summary of needs listed by priority, highest first

Need	Justification	System Effect	Solution/Approach
Mount instabilities and dark channel optics	Shifts and/or slow drift in e.g. DM mount, aft-optics frictionless zoom lenses, and 1/2" post-mounted components between measurements and after chamber loading following external alignment checks; an overly complicated imaging relay	Dark channel PSF shifting and Strehl degradation as well as chromatic aberration; reference beam tilt and path errors that can be observed on both bright and dark detectors, confounding coarse human-in-the-loop and automated fine control routines	Simplify aft-optics design, use more rugged mounts, and remove unneeded actuation – the aft-optics were redesigned in May 2016 and ruggedizing effort began in June 2016
Deformable Mirror	Amplifier to device calibration is suspected to have drifted, manifested by observed irregular (not flat) fringe pattern when the DM is set to zeroes	A subset of individual segments reach the limit of control or exhibit significant non-linear response during automated phasing and fine control	A fully-functional DM and its calibrated amplifier that have been held in reserve will be installed in the coming weeks; the DM and amplifier that have been used will be recalibrated for future use
Delay stage	Backlash error in absolute stage positioning on the order of 1–2 μm is observed using both human-in-the loop stepping and automated fringe tracking; creep is suspected	While the stroke of the PZT used for fine actuation is adequate to compensate for absolute errors, slow creep may be a source of drift away from the central null fringe during fine controls	Quantify settle time wait period needed following coarse stepper actuation before attempting fine controls; explore incorporation of a hybrid slip-stick/PZT actuated coarse/fine delay mechanism
Vacuum chamber	A limited number of access ports necessitates a six-way cross that 1) encumbers cabling and 2) introduces a torque on the system and its passive isolation	Optical mounts are subject to being inadvertently bumped or snagged during cabling – alignment checks must in some cases be repeated external to the chamber; the torque mode introduces an unwanted resonance	Ports are to be added to the chamber in the coming weeks that will enable incorporation of a connector panel for robust cable harnessing with the added benefit of yielding a more symmetric isolator load
Achromatic phase shifters	Uncoated BK7 APS were selected for the previous demonstration (TDEM-10 Milestone #2) following no-bids for multi-layer coating designs that yielded more favorable performance with a more high-purity glass option (Lithosil)	The theoretical retardance is marginally acceptable for meeting the Milestone goals, constituting a significant contribution to the leakage error budget	Fabricate a new set of APS with multiple orders of magnitude improved theoretical performance consisting of rhombs with single layer coatings on the TIR surfaces within fabrication capability; the design may enable a simplified approach to mounting that improves stability
Control OS	The Windows XP OS that has been in use exhibits bus issues and does not guarantee latency of computer operations	Communications with detectors and amplifiers periodically fail at initialization or are lost during operation and must be reset; control bandwidth is compromised	Work has begun on migrating to a system with 16 processor cores and 32 processor threads running a Linux kernel in hard realtime
Single mode fiber array	Anamorphic pitch mismatch between the SFA and its segmented DM counterpart has proven to be a difficult problem to address optically, requiring complicated relay schemes; transmission properties have yet to be characterized adequately to justify the added complexity needed for their incorporation	Complex wavefront control is performed with the DM alone, leaving segment figure errors uncorrected and no means for fine amplitude control	Characterization of several SFAs has been proposed as work to be performed in parallel to upcoming VNC efforts; if a candidate component is identified, a vacuum-compatible optical relay will be designed for their incorporation with the system

mask files used to perform wavefront control and calculate contrast be regenerated to address centroid drift or changes to platescale. An example from the previous TDEM effort is shown in Fig. 10, where over the

course of one night with no known activity in the lab, the PSF was observed to shift by $\sim 1\lambda/D$ relative to a mask that had been generated the previous day.

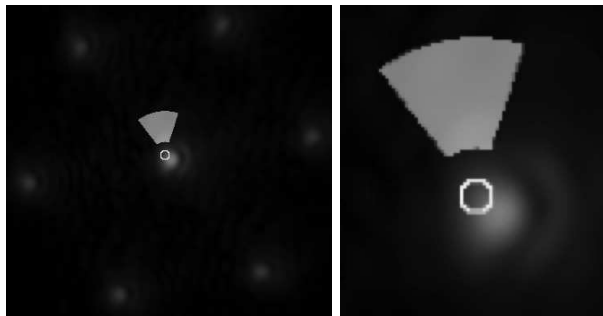


Figure 10: Analysis of the final attempt at closing the WFC loop revealed that the image had shifted on the dark detector, and therefore also relative to the predefined control mask. These figures show the location of the delay arm PSF (MMA shutter closed) relative to the location of the last measured center of the PSF for which the control mask had been generated. The $\sim 1\lambda/D$ diameter circle drawn on the data is centered on the last measured PSF center.

Adjustments to either the fore-optics or the delay line can also require modifying or generating a new MMA lookup table “flats file.” The process of array phasing is not a new issue to the system, but acquiring a “feel” for this process is something that takes time for not just a new user, but also for each MMA and its calibrated controller. In practice, generating a flats file involves significant human-in the loop interaction that can sometimes converge quickly, or at other times be very time consuming. The goal is achieve reliable constant alignment such that the flattening of the DM can be as automatic a process as possible, needing less human-in-the-loop monitoring and intervention. Simpler mounts with fewer frictional joints and larger diameter posts are being used to achieve a more stable system with the reworking of the aft-optics.

7.2 Vacuum-compatible dark channel optics

The dark channel aft-optics relaying the MMA pupil to the Lyot mask to the focal plane proved detrimental to achieving the VNC broadband Milestone #2. The aft-optics included several zoom lenses, the justification for which was to match the segment spacing of the MMA to the pitch between fibers in a single mode fiber array (SFA). The SFA is purposed with passively enable complex wavefront control, correcting both high order surface errors that are not corrected by the MMA, as well as amplitude errors via tip/tilt control of the MMA to modify the fiber coupling overlap integral and reach $< 10^{-9}$ contrast. An alternative approach to yielding comparable control is to use two DMs (not necessarily MMAs), one in a pupil, the other in an intermediate optical plane to use the Talbot effect. The attractiveness of the SFA approach that has been pursued with interferometric efforts in the past is that, being a passive component it does not require an additional amplifier and numerous signal leads that require a proportionate increase in power and introduce added complexity and failure modes.

Simultaneously demonstrating SFA and APS capabilities was not attempted in the VNC Milestone #2 effort. Instead of using an SFA, a Lyot mask was used to block the regions of non-overlap between the reference (delay) and MMA arms. The regions of non-overlap include the segment gaps, the perimeter around the MMA outermost hexagonal ring, and five non-functioning segments. Once a candidate SFA has been identified that exhibits the complex transmission and dispersion uniformity necessary to significantly improve system performance (contrast, throughput, or both), the aft optics will be modified to relay the MMA to the SFA. To begin work on this TDEM-13 Milestone #3 effort, a 1:1 relay using (vacuum-compatible) achromatic doublets has been designed and these optics have been procured and are being laid out and tested (see Fig. 11).

7.3 A fully-functional segmented DM

The Iris AO, Inc. PTT489 mirrors used by the VNC for wavefront control have improved. Previously these devices had many non-functioning segments. Now, fully active devices are being made. A new 100% yield DM with measured surface quality shown in Fig. 12 will be used in this effort.

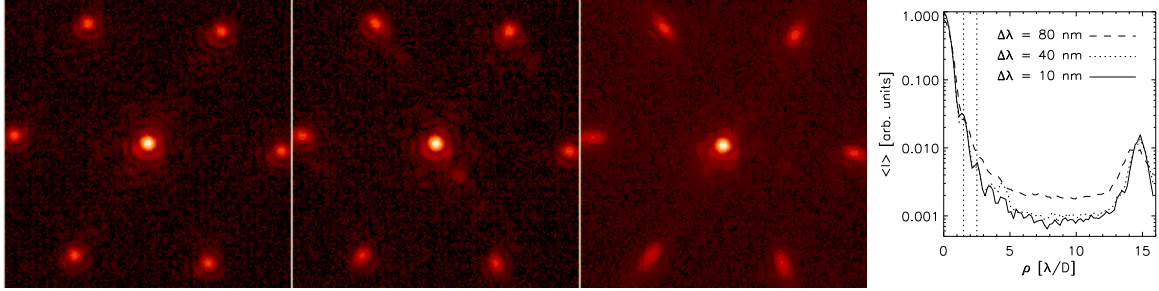


Figure 11: *From left to right:* 10, 40, and 80 nm bandpass PSFs and corresponding azimuthally-averaged profiles observed with the simplified aft optics.

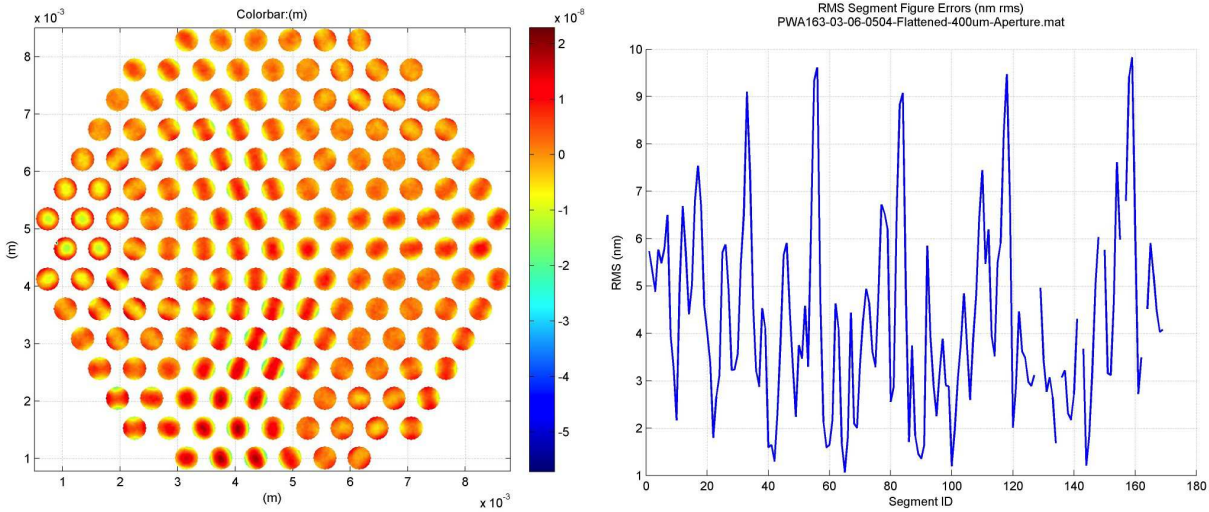


Figure 12: *Left:* Measured 400 μm circular subaperture surface data of the Iris, AO PTT489 DM that will be used in this effort. *Right:* A corresponding plot of the RMS surface error within each circular subaperture. An array of single mode fibers could be used to further reduce the correlated wavefront error over the low spatial frequencies corresponding to the dark region of highest contrast targeted by the wavefront control algorithm.[11, 7]

7.4 Delay stage stabilization

The VNC delay stage uses combined long-travel coarse stepping and 20 μm piezo-actuated linear drives. A magnet keeps the actuator stack coupled to the stage. Backlash error in absolute stage positioning on the order of 1–2 μm is observed using both human-in-the loop stepping, as well as an automated scanning approach to locate the central fringe.

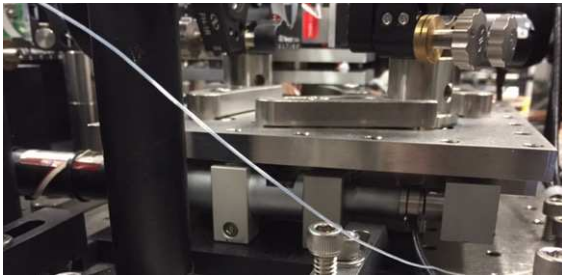


Figure 13: The VNC combined long-travel coarse stepping and 20 μm piezo-actuated linear drive delay stage. A magnet holds the stage against its actuator to minimize backlash. The stage presently holds the three mirrors and one pair of Fresnel rhombs comprising all optics in the delay arm excluding the polarizer and shutter used for amplitude balancing and calibration.

Improved routines, if not also an improved or streamlined hardware approach are needed to ensure that the

delay stage is set to zero delay between arms to minimize consumption of MMA stroke, which can lead to out-of-range conditions for individual segments. Improving the delay mechanism will become more important as MMA or DM stroke is reduced in order to improve control resolution that is limited by amplifier resolution and environmental or system electrical noise properties. A candidate long-travel replacement stage with improved absolute positioning has been identified, and funds have been allocated for procurement of this device and its controller.

7.5 Vacuum chamber modifications

A limited number of access ports on the main chamber necessitated use of a six-way cross that 1) encumbered cabling and 2) introduced a torque on the system and its passive isolation. This cabling scheme subjected optical mounts to being inadvertently bumped or snagged during cabling, which necessitated subsequent alignment checks that had to in some cases be repeated external to the chamber. The torque moment attributed to the suspended six-way is thought to have introduced an unwanted low-frequency resonance. Modifying the chamber by adding ports will address these issues.

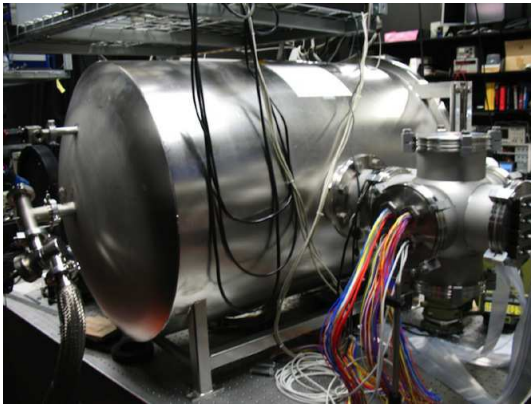


Figure 14: The VNC vacuum chamber currently has two main ports for all electrical, optical, and fluid feedthroughs, the majority of which are passed through the six-way cross added for this effort. Adding ports to the chamber will reduce the risk of damaging cables or perturbing instrument alignment, while also improving stability.

A cost and lead-time quote has been obtained for adding ports to the chamber and this work is expected to be completed in August 2016.

7.6 Enhanced Fresnel rhomb achromatic phase shifters

A solution has been identified for improving the Fresnel rhomb APS performance using a single layer of magnesium fluoride deposited on fused silica rhombs to reduce the RMS retardance variation over a given bandpass[13, 14]. The coating process can be assured by characterizing deposition on a material with a high index of refraction, e.g., sapphire or SF11, in order to measure its thickness very accurately using ellipsometry. Once the film thickness and properties are characterized, it can be deposited on high grade BK7 rhombs to generate the new rhombs using a witness for conventional characterization. The expected performance of these new rhombs that would enable broader bandpass operation is presented in Fig. 15. The theoretical chromatic leakage of this preliminary design is more than an order of magnitude less than that of the rhombs that are presently installed in the VNC.

7.7 Realtime operating system (RTOS) upgrade

The VNC control algorithms have heretofore been implemented in C/C++ with threading in a Windows XP environment. Using Windows XP as the control OS was problematic throughout the Milestone #2 effort, manifested primarily by difficulty maintaining consistent communication with the detectors and amplifiers needed for sensing and control. In the new scheme, cameras, mechanisms and the MMA will be controlled through different threads. Iris AO has provided a Linux driver for the MMA and development of multi-threaded C message passing interface (MPI) control code and work is underway to migrate the system. The goal is to increase control rates from the previous ~ 6 steps per second to > 100 steps per second. This will

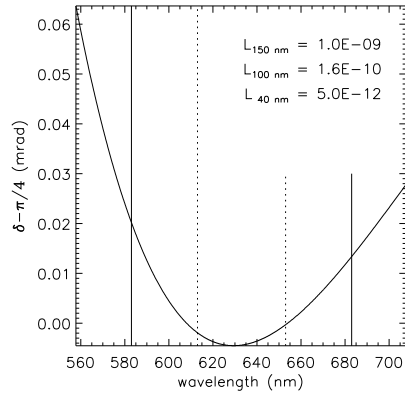


Figure 15: A BK7 APS using a single 12.7 nm thick MgF2 layer coated on each TIR surface using an angle of incidence of 51.4723 degrees. Leakages are calculated for 150, 100, and 40 nm bandpasses.

be accomplished by replacing the single processor machine that was used with a parallel processing system running 16 processor cores, 32 processor threads. Detector frame readout has already been demonstrated with the new machine using both CameraLink and USB 3.0 interfaces at rates of hundreds of frames per second in work developing the fine pointing system.

7.8 Single mode fiber array (SFA) characterization

It has been intended that a passive single mode fiber array (SFA) be used to function in concert with the tip/tilt coupling control of the MMA to actively correct wavefront amplitude errors. Each fiber is optically mapped to one MMA segment and it functions as a passive wavefront corrector. Wavefront errors at the spatial frequency scale of one cycle per MMA segment and higher are not coupled into the fiber and introduce a coupling loss.

The SFA was a jointly-funded effort between GSFC and JPL. Both funded Fiberguide Industries to develop a test unit that was delivered to GSFC in June of 2010. Separate versions of the Fiberguide units were tested at both GSFC and JPL, and both reached the conclusion that the lenslet arrays were misaligned. JPL and GSFC worked with the vendor to rectify this problem and the JPL version has now been properly aligned and separately tested at JPL. The GSFC version previously underwent realignment at Fiberguide's facility.

A set of two Agilron SFAs from were delivered to GSFC in April 2015 under SBIR Phase II Contract NNX13CG04C. Restarting an effort to characterize these newer units for use in the VNC will be undertaken pending the availability of personnel capable of performing the task. The MMA and controller used in the Milestone #1 and #2 efforts will be recalibrated and then used to perform the work needed to demonstrate complex wavefront control with candidate SFA(s) after their transmission and dispersion properties are measured.

8 Schedule

The schedule (see Fig. 16) shows a two year effort starting May 16, 2016, and culminating in final approval by the ExEP technical advisory committee on May 15, 2018. Approximately a year's worth of effort is devoted to the integration of the segmented aperture telescope with the upgraded VNC instrument, and to developing the wavefront control system and implementing it on a RTOS Linux system. These two activities will be performed in parallel. Upon complete integration of SAINT with the new control system in May, 2017, operations will begin to evaluate and refine the new wavefront control algorithms on the testbed. Contrast milestone demonstrations will be performed in late 2017-early 2018.

Reaching the SAINT Milestone goals will be accomplished incrementally, demonstrating the VNC and segmented mirror components independently. As noted in Sec. 4, a repeat demonstration of the VNC TDEM Milestone #1 narrowband performance[7] will be followed by incorporation of APS (using either the existing

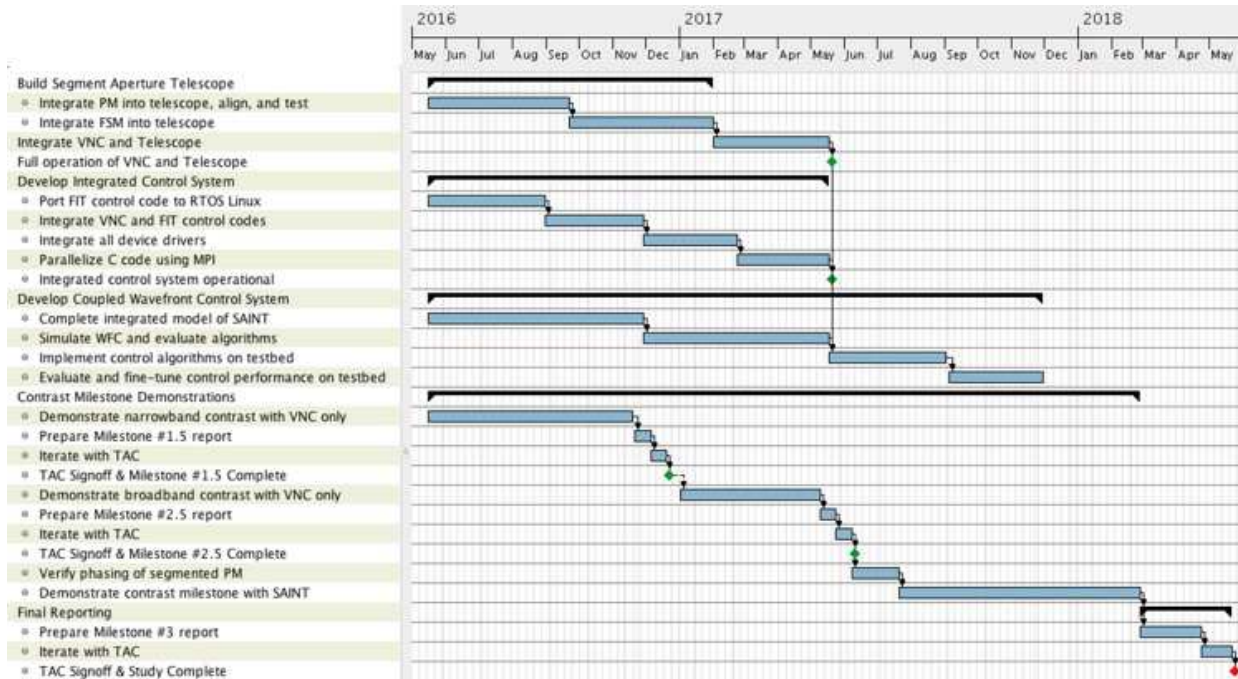


Figure 16: The SAINT TDEM-13 Schedule.

set of uncoated rhombs, or a new set of coated rhombs if available) for a broadband demonstration using the procedures and Milestone success criteria defined in the VNC TDEM Milestone #2 Final Report.[10] These intermediate Milestones as Milestone #1.5 and Milestone #2.5 along with associated Reports and TAC Reviews are noted in Fig. 16. Work to reach these preliminary goals will commence immediately, and a final demonstration of these informal milestones will be achieved late in 2017 as shown in the schedule task “Demonstrate contrast with VNC only.”

Work to build the active segmented mirror telescope component of SAINT will be completed in parallel to the preliminary demonstrations of the VNC. Performing the segmented primary work in parallel will benefit not just the VNC, but also other coronagraphic approaches undergoing development to demonstrate broadband performance at high contrast with a large segmented space telescope that might make use of the testbed.

Bibliography

- [1] C. C. Stark, A. Roberge, A. Mandell, and T. D. Robinson, “Maximizing the ExoEarth Candidate Yield from a Future Direct Imaging Mission,” *Astrophys. J.* **795**, p. 122, Nov. 2014.
- [2] M. Clampin, G. Melnick, R. Lyon, S. Kenyon, D. Sasselov, V. Tolls, H. Ford, D. Golimowski, L. Petro, G. Hartig, W. Sparks, G. Illingworth, D. Lin, S. Seager, A. Weinberger, M. Harwit, M. Marley, J. Schneider, M. Shao, M. Levine, J. Ge, and R. Woodruff, “Extrasolar planetary imaging coronagraph (EPIC),” *Proc. SPIE* **6265**, July 2006.
- [3] M. Postman, T. Brown, K. Sembach, M. Giavalisco, W. Traub, K. Stapelfeldt, D. Calzetti, W. Oegerle, R. Michael Rich, H. Phillip Stahl, J. Tumlinson, M. Mountain, R. Soummer, and T. Hyde, “Advanced Technology Large-Aperture Space Telescope: science drivers and technology developments,” *Optical Engineering* **51**, p. 011007, Jan. 2012.
- [4] M. Shao, S. Bairstow, B. Martin Levine, G. Vasisht, B. F. Lane, G. Vasudevan, R. Woodruff, R. Samuele, J. Wynn, M. Clampin, R. Lyon, and O. Guyon, “DAVINCI, a diluter aperture visible nulling coronagraphic instrument,” *Proc. SPIE* **7013**, July 2008.
- [5] R. G. Lyon, M. Clampin, R. Woodruff, G. Vasudevan, M. Shao, M. Levine, G. Melnick, V. Tolls, P. Petrone, P. Dogoda, J. Duval, and J. Ge, “Visible Nulling Coronagraphy for Exo-Planetary Detection and Characterization,” in *IAU Colloq. 200: Direct Imaging of Exoplanets: Science and Techniques*, C. Aime and F. Vakili, eds., pp. 345–352, 2006.
- [6] R. G. Lyon and M. Clampin, “Space telescope sensitivity and controls for exoplanet imaging,” *Optical Engineering* **51**, pp. 011002–011002, Jan. 2012.
- [7] M. Clampin, R. Lyon, P. Petrone III, U. Mallik, M. Bolcar, T. Madison, and M. Helmbrecht, “Visible nulling coronagraph technology maturation High contrast imaging and characterization of exoplanets,” tech. rep., NASA/Technology Development for Exoplanet Missions Final Report, JPL Document D-80950, https://exep.jpl.nasa.gov/technology/Clampin_Report_FINAL.pdf, 2013.
- [8] R. G. Lyon, K. G. Carpenter, A. Liu, P. Petrone, P. Dogoda, D. Reed, and D. Mozurkewich, “Wavefront sensing and closed-loop control for the Fizeau interferometry testbed,” *Proc. SPIE* **6687**, p. 0, Sept. 2007.
- [9] K. G. Carpenter, R. G. Lyon, C. Schrijver, M. Karovska, and D. Mozurkewich, “Direct UV/optical imaging of stellar surfaces: the Stellar Imager Vision Mission,” *Proc. SPIE* **6687**, p. 66870G, Sept. 2007.
- [10] B. Hicks, M. Bolcar, R. Lyon, M. Clampin, T. Madison, U. Mallik, P. Petrone III, and M. Helmbrecht, “Technology milestone #2 final report: Achromatic visible nulling coronagraph technology maturation,” tech. rep., NASA/Technology Development for Exoplanet Missions, JPL Document D-1547413, <https://exoplanets.nasa.gov/exep/technology/TDEM-awards/>, 2016.
- [11] R. G. Lyon, M. Clampin, P. Petrone, U. Mallik, T. Madison, and M. R. Bolcar, “High contrast vacuum nuller testbed (VNT) contrast, performance, and null control,” *Proc. SPIE* **8442**, Sept. 2012.

- [12] B. A. Hicks, R. G. Lyon, P. Petrone, I. Miller, M. R. Bolcar, M. Clampin, , M. Helmbrecht, and U. Mallik, “Demonstrating broadband billion-to-one contrast with the Visible Nulling Coronagraph,” *Proc. SPIE* **9605**, 2015.
- [13] R. J. King, “Quarter-wave retardation systems based on the Fresnel rhomb principle,” *Journal of Scientific Instruments* **43**, pp. 617–622, Sept. 1966.
- [14] P. B. Clapham, M. J. Downs, and R. J. King, “Some applications of thin films to polarization devices,” *Appl. Opt.* **8**, p. 1965, Oct. 1969.